



A novel poly (p-styrenesulfonic acid) grafted carbon nanotube/graphene oxide architecture with enhanced catalytic performance on synthesis of benzoate esters and fatty acid alkyl esters

Journal:	<i>RSC Advances</i>
Manuscript ID	RA-ART-07-2015-014813.R1
Article Type:	Paper
Date Submitted by the Author:	16-Sep-2015
Complete List of Authors:	Bian, Gang; Jiangnan University, School of Chemical and Material Engineering Jiang, Pingping; Jiangnan University, Zhang, Weijie; Jiangnan University, Jiang, Kelei; b. Wuxi WeiFu Lida Catalytic Converter CO., LTD, Hu, Ling; Jiangnan University, School of Chemical and Material Engineering Zhang, Jian; Lanzhou City University, School of Chemistry and Environmental Science; Lanzhou City University, School of Chemistry and Environmental Science Shen, Yirui; Jiangnan University, School of Chemical and Material Engineering Zhang, Pingbo; Jiangnan University, School of Chemical and Material Engineering
Subject area & keyword:	

A novel poly (p-styrenesulfonic acid) grafted carbon nanotube/graphene oxide architecture with enhanced catalytic performance on synthesis of benzoate esters and fatty acid alkyl esters

Gang Bian,^a Pingping Jiang,^{*a} Weijie Zhang,^a Kelei Jiang,^b
Ling Hu,^a Zhang Jian,^c Yirui Shen,^a and Pingbo Zhang^a

^aThe Key Laboratory of Food Colloids and Biotechnology, School of Chemical and Material Engineering,

Jiangnan University, Wuxi 214122, P.R. China. E-mail: ppjiang@jiangnan.edu.cn

^bWuxi WeiFu Lida Catalytic Converter CO., LTD, Wuxi 214177, P.R. China.

^cSchool of Chemistry and Environmental Science, Lanzhou City University, Lanzhou 730000, P.R. China.

Abstract

Considering the issue of low yield on synthesis of benzoate esters and fatty acid alkyl esters, designing a high catalytic activity composite catalyst was very significant and attractive. In this paper, rational design strategy was used to develop a novel poly (p-styrenesulfonate acid, namely PSSF) grafted multi-walled carbon nanotubes composited with graphene oxide nanomaterial (PSSF-mCNTs-GO) by a simple two-step method. FT-IR, XRD, Raman, SEM, TEM, NH₃-TPD were used to characterize this inorganic-organic hybrid material. Particularly, the addition of GO remarkably enhanced catalytic performance in the production of fatty acid alkyl esters (92.16%) and benzoate esters (90.27%), conversion was more than doubled after adding of GO, mainly due to its strong π - π interaction with substrate. Additionally, PSSF-mCNTs-GO can be separated from the substrate conveniently and still had a relatively high catalytic activity even after 6 times recycling, indicating a rather good reusability. This novel catalyst is promising in synthesis of biodiesel and benzoate esters.

1 Introduction

Among the countless esterification products, Fatty acid alkyl esters (FAAE) and benzoate esters are rather important. Fatty acid alkyl ester, called as biodiesel,^{1,2} is well-known as clean green energy and renewable liquid fuel instead of mineral fuel. Meanwhile, benzoate esters can be applied to synthesizing numbers of drug substances.³⁻⁵ Our work is mainly focusing on these two aspects.

Generally, esterification reaction is catalyzed by liquid Bronsted acids like concentrated H₂SO₄, H₃PO₄, HF, HCl, p-toluenesulfonic acid etc.⁶ Although these liquid catalysts exert rather good activity and have a moderate price, spent acid and waste water produced in esterification reaction would bring a severe problem on environmental pollution. Further, most liquid Bronsted acids⁷ belong to homogeneous catalysts, which are difficult to separate from substrates. Recently, solid acid heterogeneous catalysts⁸ are drawing researchers' attention because of their high selectivity, easy separation from the system, low emission of chemical waste liquid and low toxicity. More chemistry researchers pay attention on heteropolyacid,⁹ sulfonated ion exchange resin,¹⁰

organic-inorganic hybrid solid acid,¹¹ solid superacid¹² and SO₃H functionalized ionic liquids.¹³

In 2014, Mario et al.¹⁴ successfully applied Sn (IV)-based organometallics to the production of fatty acid alkyl esters. When the reaction temperature rose to 160°C, conversion of fatty acid with MeOH can be reached to 94% in 3 h. Additionally, In respect of benzoate esters, Wu et al.¹⁵ used SO₄²⁻/Ti₃AlC₂ ceramic as acid catalysts for esterification of benzoic acid. After 34 hours, conversion increased to 80.4%, while the catalyst amount was more than 10 wt%. Ladero's group¹⁶ also reported that an industrial free *Candida antarctica* lipase B was rather efficient in the esterification of benzoic acid with glycerol. Conversion was obtained higher than 80% when the reaction finished.

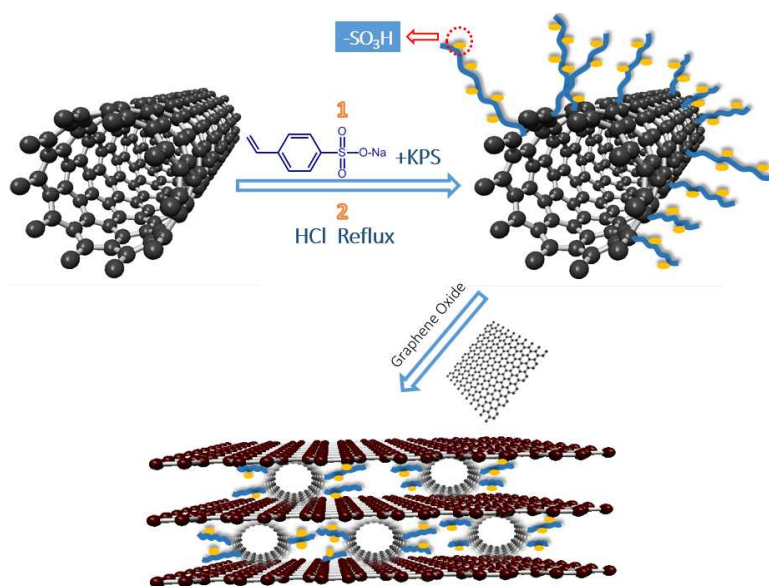
Graphene oxide (GO), since first prepared by the most classic 'Hummer's method',¹⁷ has gained considerable interest and tremendous attention due to their unique physical, chemical and electrical properties.¹⁸ During the preparation, GO was exhaustive oxidized, thus leading a containing of rich oxygen-containing functionalities like -OH, -SO₃H, -COOH, epoxide groups, etc. These abundant deficient sites endowed GO with moderate acidic and oxidizing properties.¹⁹ In addition, owing to its high surface area, GO was always used as a support to immobilize active species in catalytic reactions. As an efficient carbon-catalyst, GO has been employed into many organic acid-catalytic reactions, such as Aza-Michael addition,²⁰ Friedel-Crafts addition,²¹ hydration and oxidatio.²² Lately, Zhu et al.²³ successfully employed GO to catalyze esterification of levulinic acid with different alcohols, which finally generated alkyl levulinates. The yield of methyl levulinate could reach to as high as 99.4% only in 6h. Simultaneously, Sanny Verma et al.²⁴ pointed out GO can act as a carrier of catalyst for ester synthesis. As they reported, a magnetic nanoparticle composite was prepared by loading Pd²⁺ on the surface of GO with addition of Fe/FeO. 90% of phenylcarbinol can be catalyzed to methyl benzoate in methanol after 6 h. In summary, all the research mentioned above indicates GO a promising prospect in esterification reaction. However, Maryam et al.²⁵ presented that, in spite of the favourable catalytic activity of GO as solid acid catalyst in esterification, its reusability was unsatisfactory. The yield decreased to 14% after recycling twice. Active sites flowed away most, indicating a poor stability of GO.

Furthermore, some researchers pay attention on the effect of π - π interaction caused by GO in reactions. Li et al.²⁶ demonstrated that π - π stacking interaction between dopamine and graphene surface may accelerated the electron transfer. Jin's group²⁷ prepared a reduced graphene oxide/TiO₂ photocatalyst and proved that π - π interaction can combine the substrate with GO more tightly. Yin et al.²⁸ also found that an iron phthalocyanine can be uniformly dispersed and anchored on graphene surface with the assist of π - π stacking. Such strong interactions between substrate and graphene oxide may be beneficial for the synthesis of benzoate esters.

According to the characters of GO and problems existed above, a novel catalyst, poly (p-styrenesulfonate acid) grafted multi-walled carbon nanotubes composited with graphene oxide (PSSF-mCNTs-GO), was prepared with a two-step method. To the best of our knowledge, this is the first time to combine PSSF-mCNTs with GO and apply the catalyst into esterification reactions for synthesizing fatty acid alkyl esters and benzoate esters. Influence of chain branching degree, chain length and benzene ring with or not on catalytic activity over PSSF-mCNTs-GO had been discussed. Synthesis route was displayed in scheme 1. After examining on a series of different alcohols and acids, PSSF-mCNTs-GO was found a higher catalytic activity on aliphatic and aromatic acids with alcohols. When GO was introduced, owing to the π - π stacking interaction between GO and benzene ring, conversion of benzoate esters was more than doubled. Furthermore, PSSF-mCNTs-GO showed good reusability, there was no significant decline in catalytic activity even after six times recycling.

2 Experimental section

2.1 Synthesis of Graphene Oxide



Scheme 1. Synthesis route of PSSF-mCNTs-GO

Graphene oxide was synthesized from flake graphite (44 μm average particle diameter, Qingdao Jinrilai Graphite Co. Ltd., Qingdao, China) via a Hummers method described by Jiang Du *et al* with some Simplifications.²⁹ Briefly, flaky graphite(1.25g) and NaNO_3 (0.94g) were added into a 500mL three-necked flask. Then, concentrated H_2SO_4 (93.75mL) was slowly added with stirring in an ice-water bath. KMnO_4 (5.63g) was gradually added over 1h under vigorous stirring and kept stirring for another 2h. After keeping vigorous stirring under room temperature for 4 days, 5 wt % H_2SO_4 aqueous solution(175mL) was used to dilute the mixture over 1h., and then, kept stirring for 2h at 98°C. After the system cooling to 60°C, 30wt% H_2O_2 (7.5mL) was added in, and stirred for another 2h. When the reaction ended, the mixture we got was centrifuged and washed with 3wt% H_2SO_4 /0.5 wt% H_2O_2 aqueous solution (500mL) for 15 times. The solids at the bottom were washed with 3 wt % HCl aqueous (500mL) and one additional wash with deionized H_2O (500mL). Afterwards, the solid was dispersed again in H_2O (500mL) and ultrasonicated for 30 min. The water solution was treated with a weak basic ion-exchange resin to remove the remaining HCl acid and was centrifuged once again. Finally, the mixture (0.8g) was freezing dried for the following steps.

2.2 Preparation of PSSF-mCNTs³⁰

5.0g of sodium p-styrenesulfonate were dissolved into deionized water (200mL), with addition of 100mg mCNTs immediately. The mixture was then kept vigorous stirring for 3h after 1h high-power sonication; afterwards the mixture was transferred into a three-neck flask (1L), and 1.0g of KPS was added into as a radical initiator. To remove oxygen in the reaction, the mixture was bubbling with dry nitrogen for 1h. After the three-neck flask was placed into an oil bath, the solution was kept stirring uniformly at 80°C for 3h and 90°C for 1h subsequently.

A mixing fibroid membrane (0.45 μm) was used to filter the reaction solution when the heating process was over, the filtered black paste was washed with deionized water for 5 times using a supercentrifuge to remove the residual sodium p-styrenesulfonate. After centrifugation, the black paste was refluxed with concentrated hydrochloric acid at 120°C for 12h, and the reaction product was filtered and washed again with deionized water for 4 times using a supercentrifuge to remove the residual concentrated hydrochloric acid and sodion.

2.3 Synthesis of PSSF-mCNTs-GO nanocomposite

To form a homogeneous suspension, the as-prepared PSSF-mCNTs (100mg) and GO (50mg) were dispersed into ethanol (100mL) in a 250mL three-neck flask and followed with 2h sonication. Subsequently, the homogeneous suspension was thermal refluxed at 90°C for 2h. After the reaction, the solution was filtered and washed with deionized water for 3 times using a supercentrifuge (9000rpm) to remove ungrafted GO. Finally, the black paste was dried in a vacuum oven at 60°C overnight to get the PSSF-mCNTs-GO nanocomposite as a black solid.

2.4 Catalyst characterization

Powder X-ray diffraction (XRD) patterns were recorded on a BRUKER D8-Focus Bragg-Brentano X-ray Powder Diffractometer equipped with a Cu sealed tube ($\lambda = 1.54178\text{\AA}$) at 40 kV and 40 mA. The scanning region 2θ was from 6 to 80° with a scanning rate of 4°/min. Scanning electron microscope (SEM) investigations were carried out with a S-4800 at an accelerating voltage of 3 KV. Bright field transmission electron microscopy (TEM) images were acquired using a JEOL JEM 2100 electron microscope under an accelerating voltage of 200 KV. High-resolution transmission electron microscopy (HR-TEM) images were acquired with the same equipment of 200 KV. Samples for TEM (HR-TEM) were prepared by dispersing the powder in ethanol with ultrasonic cleaning over 1h, and then the mixed solution was dropped onto a carbon coated copper grid. Raman spectra were recorded on a confocal microscopic Raman spectrometer (Renishaw In-Via, USA) with a 532 nm laser light irradiation from 400 to 3000 cm^{-1} at a duration time of 10 s. The samples were pressed into slices before analysis. The NH_3 temperature-programmed desorption (NH_3 -TPD) measurements were conducted on an AUTO 2920 instrument (Micromeritics, USA), and a thermal conductivity detector was used for continuous monitoring of desorbed ammonia. Prior to TPD analysis, the sample was pretreated at 350°C for 1 h in a flow of ultra-pure helium gas, and the sample was cooled to 50°C. The pretreated sample was then saturated with 8% anhydrous ammonia gas for 45 min and subsequently flushed with helium gas for 1 h to remove the physisorbed ammonia. The heating rate of the TPD measurements, ranging from 50 to 800°C, was 10°C/min. Thermogravimetric analysis (TGA) was recorded using a Mettler TGA/SDTA 851 E analyzer in the temperature range 50-700 °C at a heating rate of 20 °C/min. The concentration of C, O, S and H elements in the composite catalysts have been experimentally measured by ICP emission spectrometry (Inductively Coupled Plasma) (Shimadzu ICP-7500).

2.5 Catalytic tests

The esterification catalytic tests for different acids (acetic acid, lauric acid, stearic acid, benzoic acid) with different alcohols (N-butyl alcohol, sec-butyl alcohol, tert-butyl alcohol, 1-octyl alcohol, benzyl alcohol) were carried out in a two-neck flask (25mL) with water separator under magnetic stirring. Cyclohexane was used as water-carrying agent in the esterification system. Typically, acids and alcohols (1:4, mol) with PSSF-mCNTs-GO catalyst (2 wt %) were added into the reactor and then the solution was heated to desired temperature for a specified time. The obtained product samples (draw 400 μL from the solution at 0h, 0.5h, 1h, 2h, 4h, 6h and 10 h) were separated by centrifugation and analyzed by GC. After each run, the 'used' catalyst was recycled from the reaction mixture by centrifugation and reused in sequential runs after washing with ethanol twice. Meanwhile, corrected area normalization method was used to quantify the products. Reaction temperature, time, catalyst species, substrate species were changed to investigate the dependence of main variables for comparison using the same conditions. Blank experiments (without catalyst) were also conducted as references.

3 Results and discussion

3.1 Catalyst characterization

The synthesized GO was characterized by XRD, Raman, SEM and TEM, which were showed in the supplementary information. A sharp and strong peak at 10.0° in XRD patterns (Fig.S1 A) and D band, G band as showed in Raman spectra (Fig.S1 B) all provided evidences for the formation of GO.³¹ GO presented a crumpled and layered structure from its SEM (Fig.S2 A), and TEM (Fig.S2) images revealed that the prepared GO was well-shaped. All these characters displayed in spectrograms indicated that GO would be an excellent catalyst carrier.

The successful grafting of PSSF onto mCNTs was confirmed by FT-IR and TEM. As shown in Fig.1A, after several times washing of the catalyst, the intensity of main characteristic peaks hard decreased. $-\text{SO}_3\text{H}$ exhibited a relatively weak band at 1191 cm^{-1} , which was associated with S=O stretching vibrations.³² Characteristic peaks at 1069 cm^{-1} , 620 cm^{-1} were both belong to $-\text{SO}_3^-$. Additionally, $-\text{O}-\text{H}$ which owed to $-\text{SO}_3-\text{H}$ also exhibited a strong broad band at 3435 cm^{-1} , all these characteristic peaks in FT-IR spectrum provideed a strong evidence of tight graft. To demonstrate the improved dispersy of PSSF-mCNTs compared with pristine mCNTs, the dispersy experiment dissolved in methanol was carried out (When the dispersy of catalyst improved, the active sites would dispersed better which would lead to a promotion of catalytic performance³³). Pristine mCNTs could not be well dispersed in methanol, meanwhile, it would be totally precipitated in a few minutes (Fig.1b). After grafted with PSSF, PSSF-mCNTs could be well dispersed in methanol which would form a black solution uniformly, owing to the existence of copious $-\text{SO}_3\text{H}$ groups (Fig.1b). This solution was rather stable, just a little deposition had been detected even after one month.

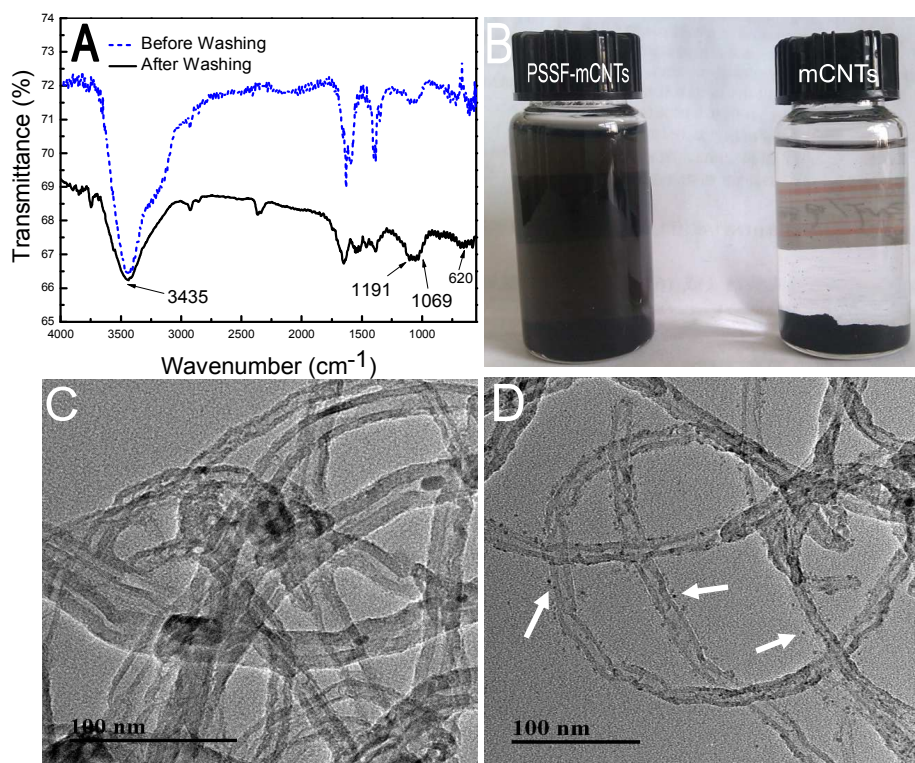


Fig.1 (A) FT-IR spectra of PSSF-mCNTs (before and after washing); (B) Dispersy experiment of PSSF-mCNTs and mCNTs in methanol; TEM images of (C) pristine mCNTs and (D) PSSF-mCNTs

Transmission electron microscopy (TEM) method was routinely deployed as an auxiliary means of characterization to realize the matters of dispersy. As can be seen in Fig.1C, due to the van der Waals attractions³⁴

between carbon nanotubes, pristine mCNTs tangled together and appeared relatively smoother. When PSSF was grafted, PSSF-mCNTs (Fig.1D) appeared better dispersity in methanol than pristine mCNTs because of the insertion of sulfonic groups. The organic groups can afford adequate electrostatic repulsions to vanquish the Van der Waals attractions.³⁵ Otherwise, around the surface of PSSF-mCNTs (Fig.1D), many small black particles which stood for poly-p-styrenesulfonate groups can be distinguished. It gave a corroborative evidence to prove the existence of $-\text{SO}_3\text{H}$ groups, which made the mCNTs much coarser.

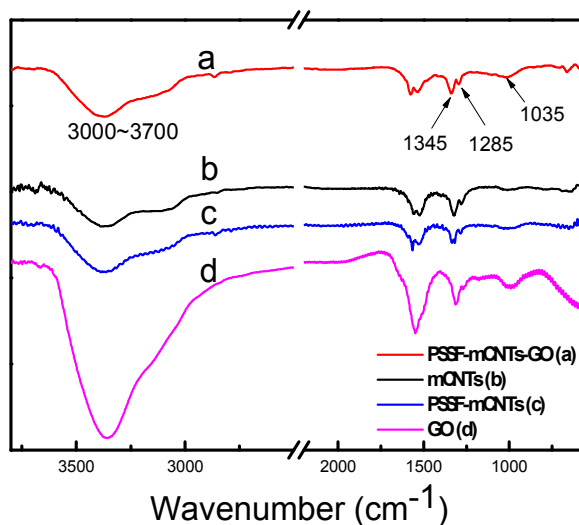


Fig.2 FTIR spectra of PSSF-mCNTs-GO (a), mCNTs (b), PSSF-mCNTs (c) and GO (d).

FT-IR, SEM and TEM were used to characterize the successful synthesized PSSF-mCNTs-GO. As shown in Fig.2, compared PSSF-mCNTs-GO with PSSF-mCNTs, the broad stretching vibration peak belonged to $-\text{OH}$ between $3000\text{--}3700\text{cm}^{-1}$ was enhanced after the doping of GO. Meanwhile, a $-\text{C}-\text{O}$ stretching vibration peak at 1285cm^{-1} owing to the carboxylic groups existed in GO was enhanced, which gave a strong evidence for the doping of GO.³⁶ Furthermore, a small sharp peak at 1345cm^{-1} associated with the $-\text{O}=\text{S}=\text{O}$ stretching vibrations and a weak band of $-\text{SO}_3^-$ symmetric stretching vibration at 1035cm^{-1} were both strengthened compared with the non-grafted GO. All these information showed in FT-IR spectrum indicated a successful graft of PSSF and a tight combination between GO and PSSF-mCNTs.

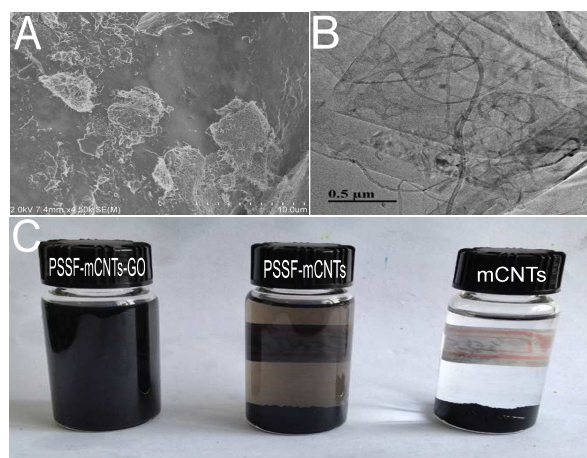


Fig.3 (A) SEM image of PSSF-mCNTs-GO (fresh); (B) TEM image of PSSF-mCNTs-GO (fresh); (C) Images of dispersity experiment of PSSF-mCNTs-GO, PSSF-mCNTs and mCNTs in methanol (3 months);

Dispersity experiment (Fig.3C) was conducted again to testify the excellent dispersity of PSSF-mCNTs-GO in methanol assisted with SEM and TEM analysis. Pristine mCNTs (Fig.3C) was totally precipitated 3 month later. Simultaneously, PSSF-mCNTs (Fig.3C) deposited most in 3 month. However, the solution containing PSSF-mCNTs-GO (Fig.3C) was quite stable, which formed a homogeneous black solution, not a little deposition was detected even after 3 month. In general, the outstanding dispersity of PSSF-mCNTs-GO provided a foundation for efficient catalysis in esterification. Similar situation was discovered in SEM and TEM images. No obvious aggregation was found in SEM image (Fig.3A) between the nanoparticles, and the carbon nanotubes were uniformly laying on the graphene oxide sheets, which matched well with the results in dispersity experiment. Carbon nanotubes interspersed randomly between the sheets of graphene oxide, leading to a further prevention of aggregation for graphene oxide nanosheets.

The NH_3 -TPD profiles were obtained for PSSF-mCNTs, PSSF-mCNTs-GO and GO at various sintering temperature (Fig.4). It can be observed that acid sites of PSSF-mCNTs and PSSF-mCNTs-GO were both located between the ranges of 100-400 $^\circ\text{C}$, which can be considered as the presence of acid sites like $-\text{SO}_3\text{H}$ with moderate strength. These results were in agreement with literature reports.^{37,38} As the calcination temperature increased to 250 $^\circ\text{C}$, the decomposition of S=O bonds happened and total acidity was rapidly decreased. Additionally, it was obvious that the peak position of PSSF-mCNTs-GO moved to high temperature direction and a stronger acidity was revealed after adding of GO, which was contributed to abundant acidic functionalities on the surface of GO such as $-\text{SO}_3\text{H}$ and $-\text{COOH}$ and the tight Van der Waals attractions between mCNTs and GO. GO in the composite catalyst not only provided a suitable substrate, but also improved the acid strength which led the enhancement of catalytic performance. These results indicated the optimum heat treatment temperature was 250 $^\circ\text{C}$ and PSSF-mCNTs-GO had more acid sites which was more beneficial to esterification reactions.

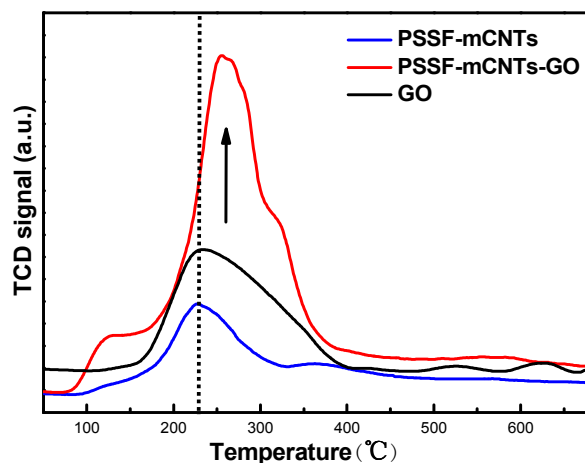


Fig.4 The profiles of temperature-programmed desorption of ammonia on PSSF-mCNTs, PSSF-mCNTs-GO and GO at various temperatures.

To further investigate the thermostability of the composite catalysts, thermogravimetric analysis (TGA) was performed on PSSF-mCNTs and PSSF-mCNTs-GO, which was displayed in supplementary information. As shown in Fig.S4, no detectable weight loss step for PSSF-mCNTs appeared before 180 $^\circ\text{C}$, and the approximate 5% weight loss before 180 $^\circ\text{C}$ of PSSF-mCNTs-GO was attributed to the physical adsorbed water. Both the PSSF-mCNTs and PSSF-mCNTs-GO had a slightly weight loss (2.61% and 9.78% respectively) between the

ranges of 180-270°C, owing to the $-\text{SO}_3\text{H}$ grafted onto the composite catalysts and abundant oxygen-containing functional groups such as $-\text{OH}$ and $-\text{COOH}$ on the surface of GO. In general, PSSF-mCNTs and PSSF-mCNTs-GO presented a considerable stability below the temperature of 180°C. As the reaction temperature was set at 120°C in the catalytic test, it was predictable that PSSF-mCNTs and PSSF-mCNTs-GO would exert a comparative catalytic stability in esterification reaction.

3.2 Catalytic activity

Reaction time and temperature had significant impact on the catalytic activity, so before the esterification, the optimum reaction time and temperature were investigated. As shown in Fig.5A, n-butanol and stearic acid were used as the probe substrates to confirm the optimum reaction time. Before time reached to 10h, conversion increased steadily over time due to the sufficient contact between reactants and catalyst. However, the conversion seldom increased after 10 hours because of the equilibrium in esterification.³⁹ Thus, we set the optimum reaction time at 10 hours for economical. Comparing to the influence of time, temperature also had a major effect on esterification conversion (Fig.5B). Before the temperature increased to 125°C, conversion increased along with the improvement of temperature, owing to the increase of thermal energy. Nevertheless, when the temperature was over 130°C, conversion began to slip down because of the volatilization of acids and alcohol. Considering lower boiling point of N-butyl alcohol, sec-butyl alcohol and tertiary butyl alcohol, we finally set the optimum reaction temperature at 120°C in esterification.

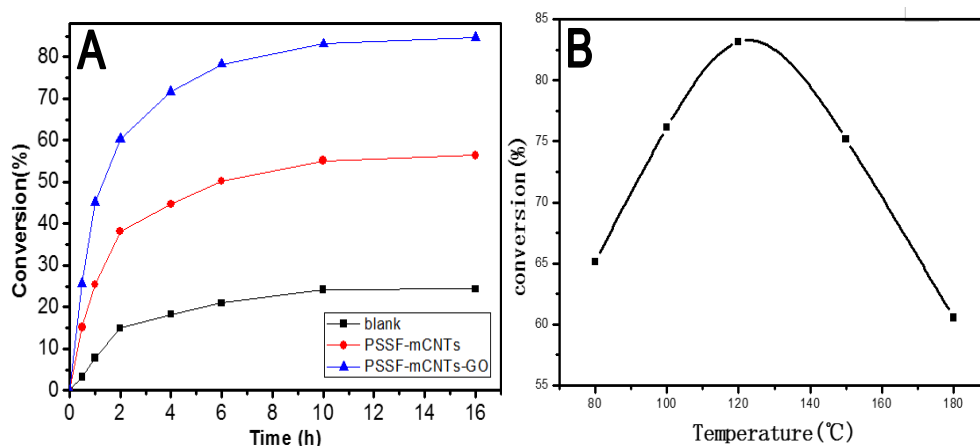


Fig.5 Effects of reaction time^a (A) and reaction temperature^a (B) in esterification.

^aReaction conditions: temperature(120°C), n-butanol: stearic acid = 4:1, catalyst amount (2 wt%)

Before the catalyst as-prepared was used in esterification, catalytic activity of PSSF-mCNTs-GO was compared with PSSF-mCNTs, concentrated H_2SO_4 and commercial catalyst (sulfonated GO), blank experiment was also conducted subsequently. As shown in Fig.6, Lauric acid and isoocetyl alcohol were taken as reaction substrates. The conversion was nearly 65.13% after 2h when PSSF-mCNTs-GO was used as the catalyst, much higher than PSSF-mCNTs (41.25%), commercial catalyst (40.56%) and concentrated H_2SO_4 (37.62%). As reacted over 10h, the PSSF-mCNTs-GO exhibited outstanding conversion (85.25%), compared with relatively low conversion of PSSF-mCNTs (65.27%), commercial catalyst (63.28%) and concentrated H_2SO_4 (58.43%). This contrast experiment proved that PSSF-mCNTs-GO was superior to similar esterification catalyst and further confirmed the prepared catalyst can act as a potential acid catalyst in industry application.

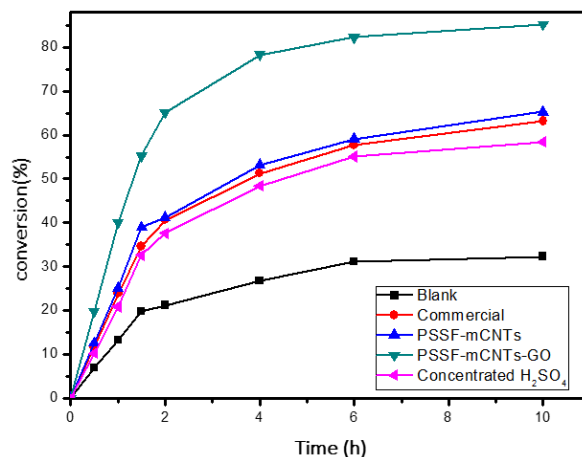


Fig. 6 Comparison of catalytic activity^a: Blank experiment (black); Concentrated H₂SO₄ (pink);

Commercial catalyst (red); PSSF-mCNTs (blue); PSSF-mCNTs-GO (green)(isooctyl alcohol:Lauric acid = 4:1)

^aReaction conditions: temperature(120°C), isooctyl alcohol:Lauric acid = 4:1, catalyst amount (2 wt%), reaction time(10h)

To test the catalytic activity of PSSF-mCNTs-GO, a series of esterification reactions were performed. The esterification catalytic tests for different acids (acetic acid, lauric acid, stearic acid, benzoic acid) with different alcohols (N-butyl alcohol, sec-butyl alcohol, tert-butyl alcohol, 1-octyl alcohol, benzyl alcohol) were provided in supplementary information (Table.S1) as comparison. All catalytic data displayed in Table.S1 indicated a promotion of conversion with the addition of GO. To further explore the rules hidden in Table.S1, three different aspects on catalytic performance were investigated.

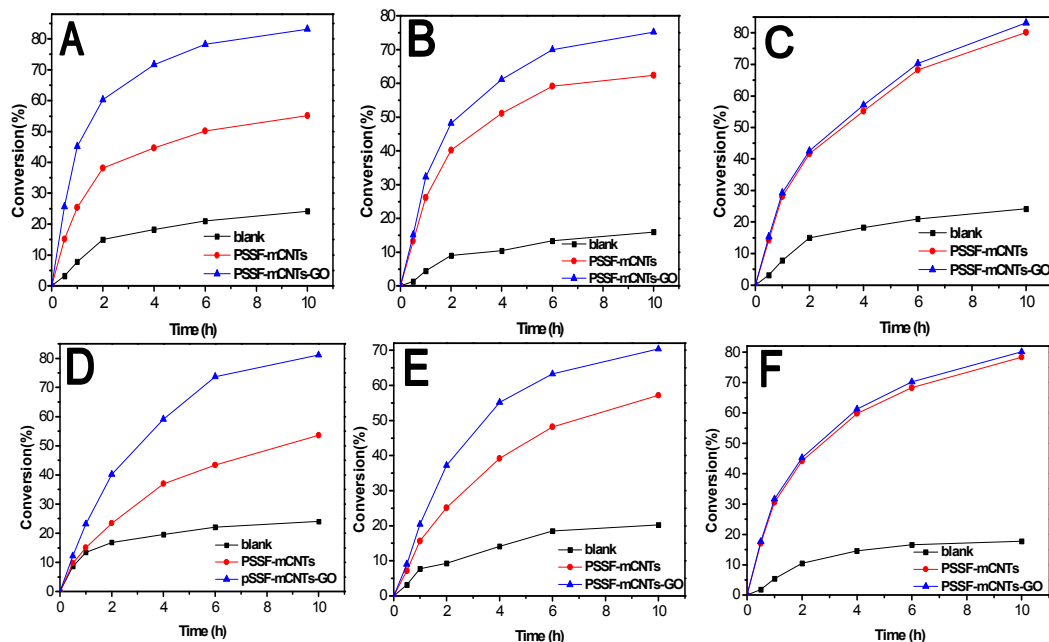


Fig. 7 Conversion of Stearic acid with different alcohols^a: A, N-butyl alcohol; B, sec-butyl alcohol; C, tertiary butyl alcohol

Conversion of lauric acid with different alcohols^a: D, N-butyl alcohol; E, sec-butyl alcohol; F, tertiary butyl alcohol

^aReaction conditions: temperature(120°C), acid: alcohol (mol, 1:4), catalyst amount (2 wt%), reaction time(10h)

First of all, catalytic performance of PSSF-mCNTs-GO in esterification with different chain branching degree alcohols was investigated. It could be seen from Fig.7 (A, B, C), when GO was combined with PSSF-mCNTs, conversion of three different alcohols with stearic acid were all increased. Interestingly, tertiary butyl alcohol turned out a better conversion (84.10%), compared with N-butyl alcohol (83.15%) and sec-butyl alcohol (75.17%). However, the catalyst without GO (PSSF-mCNTs) also exerted a rather good conversion (80.16%) to tertiary butyl alcohol, which was close to PSSF-mCNTs-GO. On the contrary, in esterification reaction of N-butyl alcohol with stearic acid, the addition of GO raised the conversion from 55.14% to 83.15%, which increased by almost 30%. The addition of GO can remarkably improve conversion of primary alcohol in esterification. The relatively high conversion of N-butyl alcohol was owed to the less steric hindrance,⁴⁰ leading the -OH exposed out, which was more beneficial for carboxy group to attack. In order to confirm the regulation we found, the same three alcohols were reacted with lauric acid subsequently. As shown in Fig.7 (D, E, F), it was found that the best catalytic activity was obtained in the esterification of N-butyl alcohol with lauric acid. Conversion was as high as 81.13%, higher than sec-butyl alcohol (70.38%) and tertiary butyl alcohol (80.16%). Likewise, the conversion of N-butyl alcohol was also greatly improved when GO was added. Hence, the above results confirmed the rule we found again that PSSF-mCNTs-GO can catalyze primary alcohol better than secondary alcohol and tertiary alcohol, which mean that the PSSF-mCNTs-GO had a higher catalytic activity for lower chain branching degree alcohols in esterification.

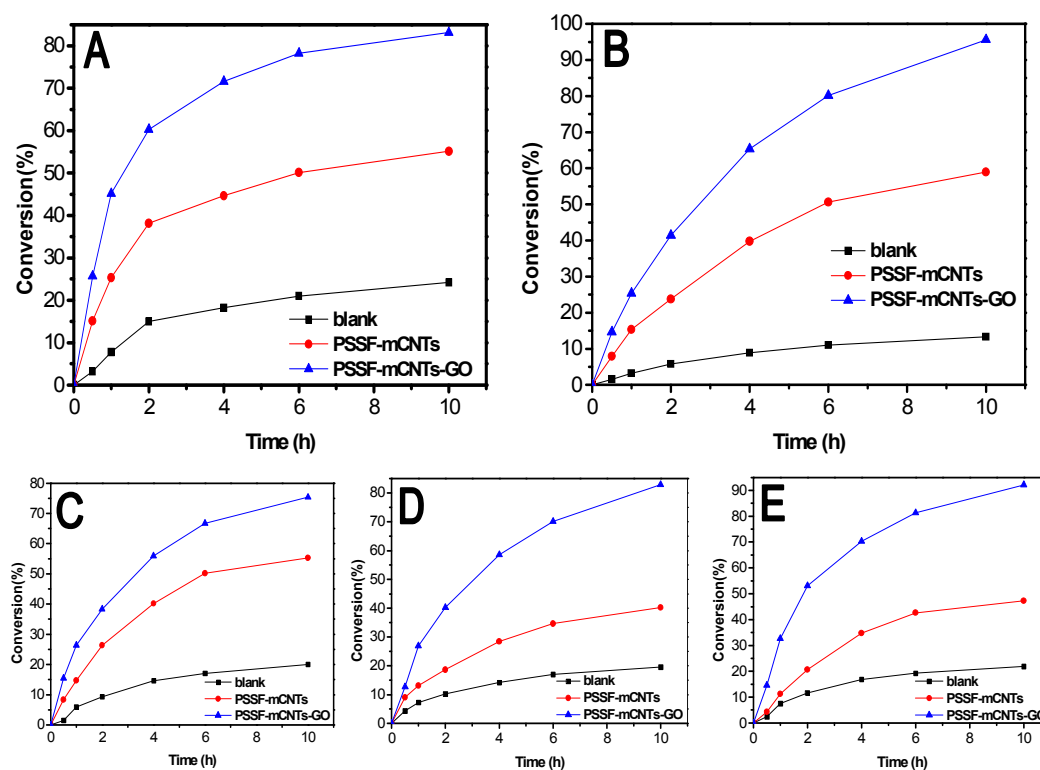


Fig.8 Conversion of stearic acid with different alcohols^a: A, N-butyl alcohol; B, 1-octanol.

Conversion of phenylcarbinol with different acids^a: C, Acetic acid; D, lauric acid; E, stearic acid

^aReaction conditions: temperature(120°C), acid: alcohol (mol, 1:4), catalyst amount (2 wt%), reaction time(10h)

In order to study the effect of chain branching degree of alcohols, catalytic activity of PSSF-mCNTs-GO for a series of alcohols and acids with different chain length was examined. As displayed in Fig.8(A, B), compared with

the short-chain n-butyl alcohol, PSSF-mCNTs-GO had a higher conversion for long chain alcohol(1-octanol), 83.15% and 95.63% respectively. Furthermore, among the acids with different chain length (acetic acid, lauric acid and stearic acid), PSSF-mCNTs-GO had the best catalytic activity for stearic acid with the longest length of carbon chain, conversion was as high as 92.16%. Especially intriguing, in the esterification of phenylcarbinol with lauric acid and stearic acid (Fig.8 D, E), PSSF-mCNTs-GO was almost twice the conversion of PSSF-mCNTs, which gave a strong evidence that addition of GO could significantly promote catalytic activity to aliphatic acids. The main reason contributed to abundant carboxyl and hydroxyl groups on the surface of GO, which was more beneficial for -OH groups exposed in aliphatic alcohols and acids to attack, thus leading to a promotion on conversion. Experimental data displayed above all ideally demonstrated PSSF-mCNTs-GO can catalyze fatty acids and alcohols in esterification well. Meanwhile, it showed potential application in preparation of biodiesel.

Further, In comparison with fatty acids, the acid substrate was extended to aromatic acids to test the catalytic activity of PSSF-mCNTs-GO. As can be seen in Fig.9 (A, B), although conversion of n-butyl alcohol and benzyl alcohol was almost the same in 10h, the conversion of benzyl alcohol raised more (40.26% to 82.93%) than n-butyl alcohol (53.60% to 81.13%) when GO existed. The same regularity was showed again in Fig.9 (C, D), not only conversion of benzoic acid (90.27%) was higher than acetic acid (70.15%), but also the conversion enhanced from 40.68% to 90.27% with the addition of GO, which was more than doubled, catalytic activity was significantly improved. Such strong catalytic activity for benzoate esters was contributed to the conjugation between the sp² hybrid C atom of graphene oxide surface and delocalized pi bond in benzene ring.^{41,42} The π - π stacking interaction can accelerate the electron transfer between catalyst and reactants⁴³, thus leading to a substantial promotion of catalytic activity.

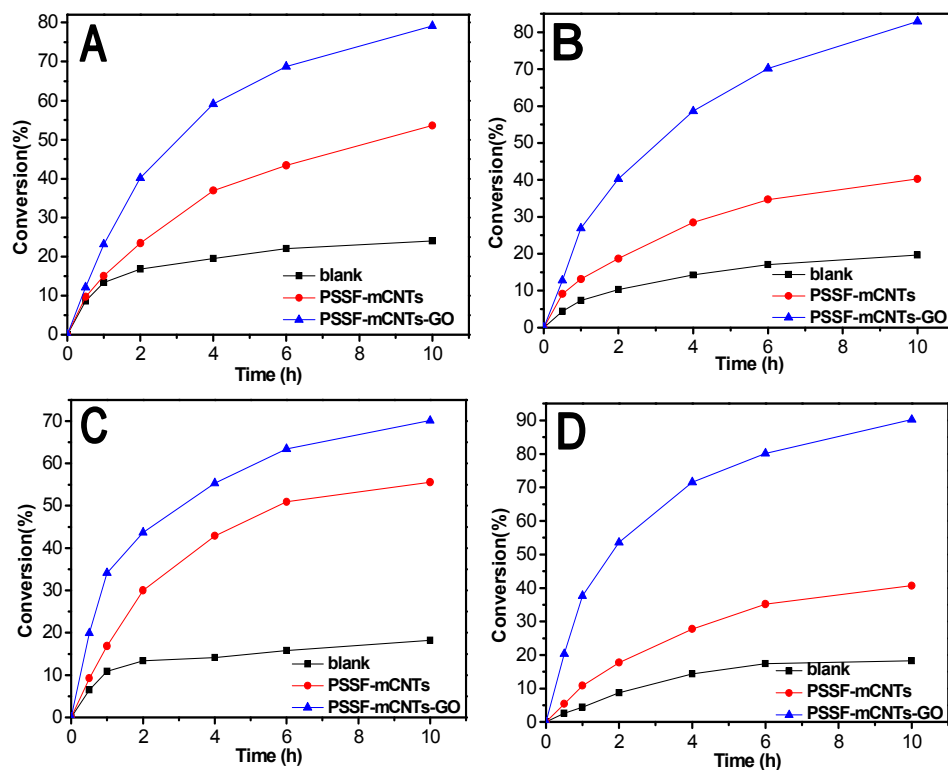


Fig. 9 Conversion of lauric acid with different alcohols^a: a, N-butyl alcohol; b, phenylcarbinol.

Conversion of N-butyl alcohol with different acids^a: c, Acetic acid; d, benzoic acid

^aReaction conditions: temperature(120 °C), acid: alcohol (mol, 1:4), catalyst amount (2 wt%), reaction time(10 h)

Reusability of PSSF-mCNTs-GO was measured (Fig.10). The 'used' catalyst was recycled by centrifugation and then reused. Even after 6 times recycling, a slightly decline of conversion was detected, catalytic activity was almost consistent. Furthermore, to demonstrate such high structure stability of PSSF-mCNTs-GO in catalytic reactions and illustrate the change of $-SO_3H$ content between the fresh and recycled catalyst, SEM, TEM and ICP analysis were carried out to confirm the structure of PSSF-mCNTs-GO and characterize the S element content in the composite catalyst, respectively. No obvious change was observed through a comparison of Fig.3 (A, B) and Fig.S5 (A, B), the recycled catalyst still maintain a similar morphology after recycling 6 times. Meanwhile, as shown in Table.S2, there was no significant change of S element content between fresh and recycled catalyst, which indicated the as-prepared catalyst was quite stable in esterification reactions.

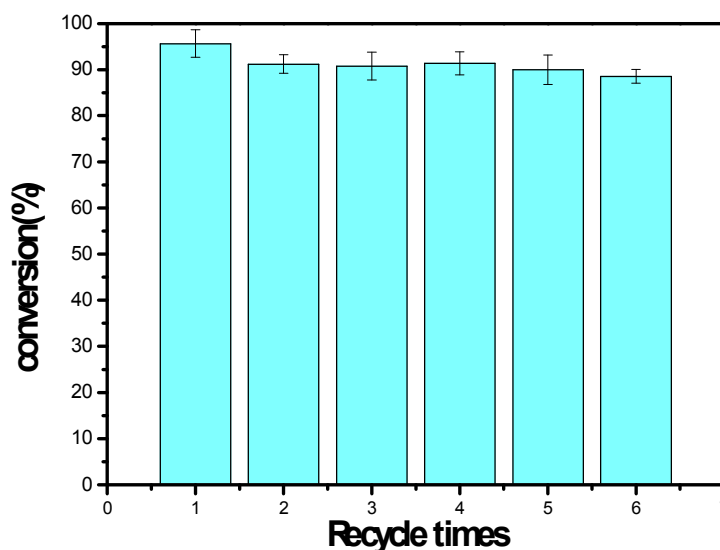


Fig.10 The cycling experiment of catalytic activity ^a

^aReaction conditions: temperature(120°C), 1-octyl alcohol: stearic acid=4:1, PSSF-mCNTs-GO amount (2 wt%), reaction time(10h)

4. Conclusion

Compared to conventional solid acid catalyst, PSSF-mCNTs-GO prepared with a two-step method showed a good catalytic stability and was proved to be high active acid catalyst towards the esterification of fatty and aromatic acids with alcohols. After adding of GO with appropriate amount in the composite catalyst, the catalytic activity was significantly increased. In particular, conversion of aliphatic (stearic acid) and aromatic acid (benzoic acid) in the esterification reactions was more than doubled, they were as high as 92.16% and 90.27%, respectively. Additionally, π - π stacking interaction between benzene ring and graphene oxide was more beneficial for the synthesis of benzoate esters. Otherwise, no significant decline in catalytic activity was found even after recycling six times. It's worth mentioning that such a robust solid acid catalyst held great potential on synthesis of biodiesel and aromatic esters. However, more studies are still needed to explore the mechanism of such high conversion and a deep understanding of graphene-supported solid acids would be acquired.

Acknowledgements

The authors gratefully acknowledge the financial support from National "Twelfth Five-Year" Plan for Science & Technology (2012BAD32B03), the Fundamental Research Funds for the Central Universities (JUSRP51507) and the Postgraduate Innovation Project of Jiangsu Province (KYLX15-1156).

Notes and references

- 1 Ma F, Hanna M A. *Bioresource technology*, 1999, 70(1): 1-15.
- 2 Hoekman S K, Broch A, Robbins C, et al. *Renewable and Sustainable Energy Reviews*, 2012, 16(1): 143-169.
- 3 X. Li, W. Eli, G. Li, *Catalysis Communications*, 2008, 9(13): 2264-2268.
- 4 Barbosa S L, Hurtado G R, Klein S I, et al. *Applied Catalysis A: General*, 2008, 338(1): 9-13.
- 5 Shi H, Zhu W, Li H, et al. Microwave-accelerated esterification of salicylic acid using Brønsted acidic ionic liquids as catalysts[J]. *Catalysis Communications*, 2010, 11(7): 588-591.
- 6 (a) A. Sakakura, Y. Koshikari and K. Ishihara, *Tetrahedron Lett*, 2008, 49, 5017–5020.
(b) K. Ishihara, *Tetrahedron*, 2009, 65, 1085–1109
- 7 Stoyanov E S, Hoffmann S P, Juhasz M, et al. *Journal of the American Chemical Society*, 2006, 128(10): 3160-3161.
- 8 Melero J A, Iglesias J, Morales G. *Green Chemistry*, 2009, 11(9): 1285-1308.
- 9 Su F, An S, Song D, et al. *Journal of Materials Chemistry A*, 2014, 2(34): 14127-14138.
- 10 Ma L, Han Y, Sun K, et al. *Energy Conversion and Management*, 2015, 98: 46-53.
- 11 Zhang Z, Dong K, Zhao Z K. *ChemSusChem*, 2011, 4(1): 112-118.
- 12 Li Y, Zhang X D, Sun L, et al. *Applied Energy*, 2010, 87(1): 156-159.
- 13 Hengne A M, Kamble S B, Rode C V. *Green Chemistry*, 2013, 15(9): 2540-2547.
- 14 Meneghetti M R, Meneghetti S M P. *Catalysis Science & Technology*, 2015, 5(2): 765-771.
- 15 Wu M, Guo J, Li Y, et al. *Ceramics International*, 2013, 39(8): 9731-9736.
- 16 Tamayo J J, Ladero M, Santos V E, et al. *Process Biochemistry*, 2012, 47(2): 243-250.
- 17 Offeman R E, Hummers W S. *J Am Chem Soc*, 1958, 80: 1339-1339.
- 18 Zhu Y, Murali S, Cai W, et al. *Advanced materials*, 2010, 22(35): 3906-3924.
- 19 D.R. Dreyer, H.-P. Jia, C.W. Bielawski, *Angew. Chem. Int. Ed.* 122 (2010) 6965–6968.
- 20 Verma S, Mungse H P, Kumar N, et al. *Chem. Commun.*, 2011, 47(47): 12673-12675.
- 21 Kumar A V, Rao K R. *Tetrahedron Letters*, 2011, 52(40): 5188-5191.
- 22 Dreyer D R, Jia H P, Bielawski C W. *Angewandte Chemie*, 2010, 122(38): 6965-6968.
- 23 Zhu S, Chen C, Xue Y, et al. *ChemCatChem*, 2014, 6(11): 3080-3083.
- 24 Verma S, Verma D, Sinha A K, et al. *Applied Catalysis A: General*, 2015, 489: 17-23.
- 25 Mirza-Aghayan M, Boukherroub R, Rahimifard M. *Turk J Chem*, 2014, 38: 859-864.
- 26 Wang Y, Li Y, Tang L, et al. *Electrochemistry Communications*, 2009, 11(4): 889-892.
- 27 Joseph K L V, Lim J, Anthonysamy A, et al. *Journal of Materials Chemistry A*, 2015, 3(1): 232-239.
- 28 Yin H, Zhang C, Liu F, et al. *Advanced Functional Materials*, 2014, 24(20): 2930-2937.
- 29 Du J, Lai X, Yang N, et al. *ACS nano*, 2010, 5(1): 590-596.
- 30 Zhang X H, Tang Q Q, Yang D, et al. *Materials Chemistry and Physics*, 2011, 126(1): 310-313.
- 31 Y. Wang, I. Djerdj, B. Smarsly, M. Antonietti, *Chemistry of Materials* 2009, 21, 3202-3209.
- 32 Liu F, Sun J, Zhu L, et al. *Journal of Materials Chemistry*, 2012, 22(12): 5495-5502.
- 33 Du G, Lim S, Pinault M, et al. *Journal of Catalysis*, 2008, 253(1): 74-90.
- 34 Li C, Chou T W. *Composites Science and Technology*, 2003, 63(11): 1517-1524.
- 35 Price S L, Stone A J. *The Journal of chemical physics*, 1987, 86(5): 2859-2868.
- 36 Stankovich S, Dikin D A, Piner R D, et al. *Carbon*, 2007, 45(7): 1558-1565.
- 37 Xiao G, Zhou J, Huang X, et al. *RSC Advances*, 2014, 4(8): 4010-4019.
- 38 Zhao H, Jiang P, Dong Y, et al. *New Journal of Chemistry*, 2014, 38(9): 4541-4548
- 39 Chin S Y, Ahmad M A A, Kamaruzaman M R, et al. *Chemical Engineering Science*, 2015, 129: 116-125.

- 40 Taherimehr M, Sertã J P C C, Kleij A W, et al. *ChemSusChem*, 2015, 8(6): 1034-1042.
- 41 Novoselov K S, Geim A K, Morozov S V, et al. *science*, 2004, 306(5696): 666-669.
- 42 Meng F L, Li H H, Kong L T, et al. *Analytica chimica acta*, 2012, 736: 100-107.
- 43 Vlček Jr A, Kvapilová H, Towrie M, et al. *Accounts of chemical research*, 2015, 48(3): 868-876.

Graphic abstract

